International Journal of Biological, Life and Agricultural Sciences
ISSN: 2415-6612
Vol:4, No:8, 2010

X-ray Crystallographic Analysis of MinC N-Terminal Domain from *Escherichia coli*

Jun Yop An, Kyoung Ryoung Park, Jung-Gyu Lee, Hyung-Seop Youn,Jung-Yeon Kang, Gil Bu Kang and Soo Hyun Eom

***Abstract*—**MinC plays an important role in bacterial cell division system by inhibiting FtsZ assembly. However, the molecular mechanism of the action is poorly understood. *E. coli* MinC N-terminus domain was purified and crystallized using 1.4 M sodium citrate pH 6.5 as a precipitant. X-ray diffraction data was collected and processed to 2.3 Å from a native crystal. The crystal belonged to space group $P2_12_12_1$, with the unit cell parameters a = 52.7, b = 54.0, c = 64.7 Å. Assuming the presence of two molecules in the asymmetric unit, the Matthews coefficient value is 1.94 $Å^3$ Da^{-1}, which corresponds to a solvent content of 36.5%. The overall structure of $MinC^N$ is observed as a dimer form through anti-parallel ß-strand interaction.

***Keywords*—**MinC, Cell division, Crystallization.

I. Introduction

IN bacteria, cytokinesis is controlled by cytokinetic ring, called as the Z-ring, which recruits other cell-division proteins [1]-[3]. Z-ring consists of FtsZ filaments and is normally located at the midcell in cell division by attaching to the membrane through membrane-associated proteins ZipA and FtsA. However, Z-ring is not limited to midcell and also occurs near the cell polar region in the absence of the *min* system [4]. Successful cell division in *Escherichia coli* requires the mutual cooperative action of the Min proteins, MinC, MinD and MinE [5]-[6]. MinC interacts with MinD to become a division inhibitor that block polar division by destabilizing FtsZ polymers at polar region while oscillating from one polar region to the other polar region in a cell [7]-[8]. MinD concentrates MinC at the membrane, which enhances the inhibitory activity of MinC up to 50-fold [9, 10]. However, MinE inhibits MinCD by dissociating the MinCD complex near the midcell division site to prevent the disassembly of FtsZ polymers [11]-[12]. Based on these behaviors between Min proteins, Z-ring is stably positioned at the midcell division site and a cell could be equally divided into two daughter cells.

MinC is composed of two functional domains, which are both of N-terminal domain ($MinC^N$) that blocks FtsZ assembly and C-terminal domain ($MinC^C$) that interacts with MinD and binds to FtsZ to antagonize the bundling of FtsZ filaments as well [13]-[15]. Thus, the studies on MinC affecting FtsZ assembly have been actively reported. Nevertheless, the molecular mechanism of MinC that inhibits FtsZ assembly hasn't been understood yet. Currently, only two MinC structures have been known. Reported crystal structures of full length MinC from *T. maritima* (PDB code 1hf2) and $MinC^N$ from *S. typhimurium* (PDB code 3ghf) show different dimerization mode. To provide structural evidence underlying dimer interaction by the $MinC^N$ from *E. coli* as a model system, we purified and crystallized the dimeric $MinC^N$ from *E. coli*.

All authors are with Department of Life science, Gwangju Institute of Science and Technology, Gwangju 500-712, South Korea (Corresponding author to e-mail: eom@gist.ac.kr)

II. Materials And Methods

Expression and purification

The recombinant gene was cloned from *E. coli* (ATCC No.700926D-5) genomic DNA by PCR technique using the primer pair (5′-GTC AAC GGA TCC ATG TCA AAC ACG CC-3′ and reverse primer 5′-CCC TTC CTC GAG **TCA** CGC TTT TTC CTT-3′), where underlined letters indicate nucleotide that were introduced to generate the restriction sites and the end codon is described as bold letters. The DNA was inserted into the modified pET-28a vector using *BamH*I/*Xho*I site. The recombinant plasmid was transformed into *E. coli* strain BL21 (DE3) for overexpression of protein. The cells were grown in LB medium using 50 μg/ml kanamycin at 310 K until OD_{600} reached approximately 0.7 and expression of the recombinant protein was induced by the addition of 0.5 mM Isopropyl β-D-1-thiogalactopyranoside (IPTG) followed by 9 h incubation at the same temperature. The cells were obtained by centrifugating at 4,500*g* for 15 min at 277 K. The cell pellet was resuspended with buffer A containing (50 mM sodium phosphate pH 8.0, 300 mM NaCl, 5 mM imidazole) and lysed by sonication. The crude lysate was centrifuged at 16,000*g* for 50 min at 277 K. The supernatant was loaded onto a Ni-NTA resin (Peptron) that had been previously equilibrated and washed with buffer A. The protein was eluted with buffer B containing (50 mM sodium phosphate pH 8.0, 300 mM NaCl, 300 mM imidazole). The eluate was concentrated using Centriprep YM-3 (Millipore) and size exclusion chromatography was performed with Superdex 200 16/60 column (GE Healthcare, USA) that had been equilibrated with buffer C containing (20 mM Tris-HCl pH 8.0, 150 mM NaCl, 1 mM DTT). The eluates were finally concentrated to 14 mg/ml with Centriprep YM-3 (Millipore) for crystallization.

Crystallization and X-ray analysis

Initial crystallization trial was performed with Crystal screen I and II (Hampton Research, USA). Crystallization conditions were further refined by the hanging-drop vapor-diffusion method at 294 K, mixing 1 μl of protein solution with 1 μl of reservoir solution.

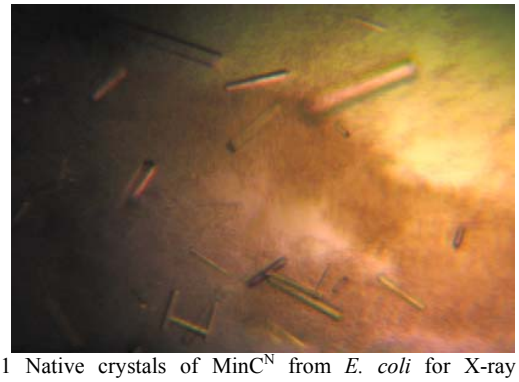

Fig. 1 Native crystals of $MinC^N$ from *E. coli* for X-ray data-collection. The maximum dimensions of crystal are approximately 0.05 × 0.05 × 0.3 mm.

The best crystals were observed after 3 days in reservoir solution consists of 1.4 M sodium citrate pH 6.5 (Figure 1). The crystal was immersed into paratone as a cryoprotectant before flash-freezing in liquid nitrogen for X-ray diffraction experiment. X-ray diffraction data was collected on beamline 4A (MXW) of the Pohang Accelerator Laboratory (Pohang, South Korea). The crystal-to-detector distance was set to 300 mm and a total of 300 images were recorded with an oscillation angle of 1.0°, an exposure time of 10 seconds per image and a wavelength of 1.0000 Å. The data set(Table 1) was processed and scaled using *HKL*-2000 [16].

Structure determination and refinement

The native crystal has space group $P2_12_12_1$ and unit cell parameter a = 52.7, b = 54.0, c = 64.7 Å. Assuming the presence of two molecules in the asymmetric unit, the calculated Matthews coefficient value is 1.94 $Å^3$ Da^{-1}, which corresponds to a solvent content of 36.5% [17]. The crystal structure of *E. coli* $MinC^N$ was solved by the molecular-replacement method using the program PHASER [18] with that of *Salmonella typhimurium* MinC (PDB code 3ghf) as a search model. To Refine the structure of *E. coli* $MinC^N$, Many cycles of manual rebuilding using the program COOT[19] and refinement using the program CNS[20] and Refmac 5[21] were performed (Table 1).

III. Results and Discussion

Overall structure of $MinC^N$

The structure of MinC N-terminal domain has been solve by MR method using that of *Salmonella typhimurium* MinC (PDB code 3ghf) as a search model. The final R value is refined to an R_{work} = 24%, R_{free} = 27.4%. After determining the structure, it has been shown that the overall structure is a dimer form that is associated with each other through anti-parallel ß-strand interaction, which is correlated with that size-exclusion chromatography showed that $MinC^N$ forms a stable dimer in buffer solution (data not shown). Monomer of $MinC^N$ has three α-helices which are composed of α1 (residues 25-43), α2 (residues 61-71), α3 (residues 84-93) and a three-stranded ß sheet that consist of ß1 (residues 6-20), ß2 (residues 47-51), ß3 (residues 77-79).

Putative polymer model structure of MinC

Bacterial cell has an unqiue cell division system to do identical cell division. Z-ring is located to mid-site to perfom properly the cell division. But, Z- ring also can move to polar zones. MinC inhibits Z-ring near polar zones to prevent the result in a cell. In that point, MinC plays a important role in Z-ring mid-position. As mentioned above, the structure of $MinC^N$ has been revealed as a dimer. Based on the aspect of $MinC^N$ interactions, we could think that individual MinC molecules are strongly associated with each other through N-terminal domain when MinC polymer should be formed (Figure 3). And it would be thought that dimer of $MinC^N$ is a effective form to fufill optimally because $MinC^N$ would carry out the work by grabbing interfaces between subunits when MinC should attack the longitudinal bond between FtsZ subunits to perform its role. Additionally, it is associated with each other through anti-parallel ß-strand interaction , which means mighty connection. Therefore, it would be stably maintained as dimer form regardless of that the interface between $MinC^N$ are opened or closed even though plenty of motility occurs to inhibit Z-ring.

Acknowledgment

We thank Drs. Kyung-Jin Kim, and Yeon-Gil Kim for their kind support with X-ray data collection at BL-4A of Pohang Accelerator Laboratory (Pohang, Korea). This work was supported by grants from the Cell Dynamics Research Center at GIST (R11-2007-007-03001-0).

References

[1] Lutkenhaus, J. "Assembly dynamics of the bacterial MinCDE system and spatial regulation of the Z ring", (2007). Annu. Rev. Biochem., 76, 539-562.
[2] Dajkovic, A. and Lutkenhaus, J. "Z ring as executor of bacterial cell division", (2006) J. Mol. Microbiol. Biotechnol., 11, 140-151.
[3] Lutkenhaus, J. "The regulation of bacterial cell division: a time and place for it", (1998) Curr. Opin. Microbiol., 1, 210-215.
[4] Yu, X.-C. and Margolin, W. "FtsZ ring clusters in min and partition mutants: role of both the Min system and the nucleoid in regulating FtsZ ring localization", (1999) Mol. Microbiol., 32, 315-326.
[5] de Boer, P. A., Crossley, R. E. and Rothfield, L. I. "A division inhibitor and a topological specificity factor coded for by the minicell locus determine proper placement of the division septum in E. coli", (1989) Cell, 56, 641-649.
[6] Rothfield, L., Justice, S. and Garcia-Lara, J." Bacterial cell division", (1999) Annu. Rev. Genet., 33, 423-448.
[7] Hu, Z. and Lutkenhaus, J. "Topological regulation of cell division in Escherichia coli involves rapid pole to pole oscillation of the division inhibitor MinC under the control of MinD and MinE", (1999) Mol. Microbiol., 34, 82-90.
[8] Raskin, D. M. and de Boer, P. A. "Rapid pole-to-pole oscillation of a protein required for directing division to the middle of Escherichia coli", (1999) Proc. Natl. Acad. Sci USA, 96, 4971-4976.
[9] Hu, Z., Mukherjee, A., Pichoff, S. and Lutkenhaus, J. "The MinC component of the division site selection system in Escherichia coli interacts with FtsZ to prevent polymerization", (1999) Proc. Natl. Acad. Sci. USA, 96, 14819-14824.
[10] Raskin, D. M. and de Boer, P. A. "MinDE-dependent pole-to-pole oscillation of division inhibitor MinC in Escherichia coli", (1999) J. Bacteriol., 181, 6419-6424.
[11] Huang, J., Cao, C. and Lutkenhaus, J. "Interaction between FtsZ and inhibitors of cell division", (1996) J. Bacteriol., 178, 5080-5085.

[12] King, G. F., Shih, Y. L., Maciejewski, M. W., Bains, N. P., Pan, B., Rowland, S. L., Mullen, G. P. and Rothfield, L. I. "Structural basis for the topological specificity function of MinE", (2000) Nat. Struct. Biol., 7, 1013-1017.
[13] Shen, B. and Lutkenhaus, J. "The conserved C-terminal tail of FtsZ is required for the septal localization and division inhibitory activity of MinC(C)/MinD", (2009) Mol. Microbiol., 72, 410-424.
[14] Dajkovic, A., Lan, G., Sun, S. X., Wirtz, D. and Lutkenhaus, J. "MinC spatially controls bacterial cytokinesis by antagonizing the scaffolding function of FtsZ", (2008) Curr. Biol., 18, 235-244.
[15] Hu, Z. and Lutkenhaus, J. "Analysis of MinC reveals two independent domains involved in interaction with MinD and FtsZ", (2000) J. Bacteriol., 182, 3965-3971.
[16] Otwinowski, Z. and Minor, W. "Processing of X-ray diffraction data collected in the oscillation mode", (1997) Methods Enzymol., 276, 307-326.
[17] Matthews, B. W. "Solvent content of protein crystals", (1968) J. Mol. Biol., 33, 491-497.
[18] McCoy, A. J., Grosse-Kunstleve R. W., Storoni, L. C. and Read, R. J. "Likelihood-enhanced fast translation functions", (2005) Acta Crystallogr. D. Biol. Crystallogr., 61, 458-464.
[19] Emsley, P. & Cowtan, K. "Coot: model-building tools for molecular graphics", (2004) Acta Crystallogr. D., 60, 2126–2132.
[20] Brünger, A. T., Adams, P. D., Clore, G. M., Delano, W. L., Gros, P., Grosse-Kunstleve, R. W. et al. "Crystallography and NMR systems: a new software suite for macromolecular structure determination", (1998)Acta Crystallogr. D., 54, 905–921.
[21] Murshudov, G. N.,Vagin, A.A. and Dodson,E.J. "Refinement of macromolecular structures by the maximum-likelihood method", (1997) Acta Crystallogr. D., 53, 240–255.

TABLE I
DATA COLLECTION AND REFINEMENT STATISTICS FOR *E.COLI* MINC^N

Dataset	MinC^N
X-ray source	PAL-4A
Wavelength (Å)	1.0000
Space group	$P2_12_12_1$
Unit cell dimensions (Å)	a =52.7, b=54.0, c=64.7
Resolution (Å) [a]	50-2.30 [2.34-2.30]
Observed reflections	99925
Unique reflections	8799
Multiplicity	11.3 [10.2]
Completeness (%)	99.8 [98.8]
R_{merge} [b] (%)	6.5 [41.5]
$I/\sigma(I)$	13.8 [4.6]
Refinement	
R_{work} [c] total (%)	24
R_{free} [d] total (%)	27.4
R.m.s. bond length (Å)	0.008
R.m.s. bond angle (°)	1.7
Average B value (Å2)	52.1

[a] Values in brackets are for the highest resolution shell.
[b] $R_{merge} = \sum_{hkl}\sum_i |I_i(hkl) - \langle I(hkl)\rangle| / \sum_{hkl}\sum_i I_i(hkl)$, where $I_i(hkl)$ is the intensity of the ith observation of reflection hkl and $\langle I(hkl)\rangle$ is the average intensity of reflection hkl.
[c] Rwork = Σ ‖Fo| - |Fc‖ /Σ|Fo|.
[d] Rfree calculated with 10% of all reflections excluded from refinement stages using high resolution data.

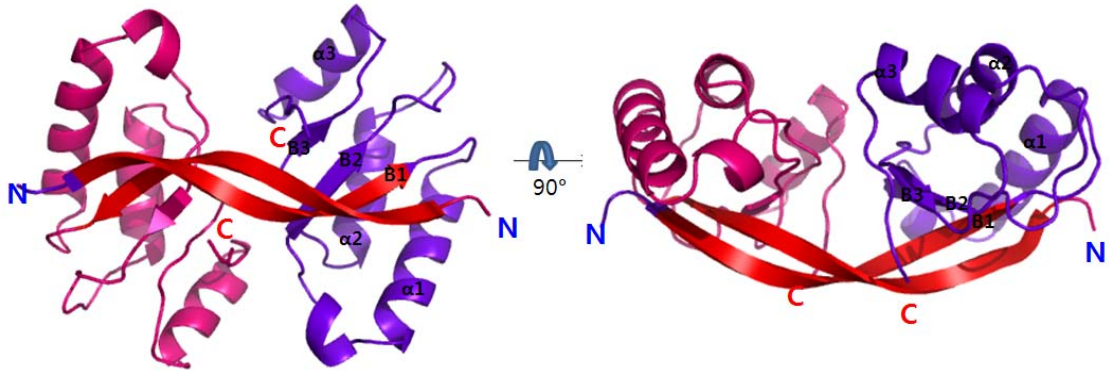

Fig. 2 Structure of MinC^N from *E. coli*. N-terminal domains are connected to each other through anti-parallel ß-strand interaction. Each monomer consists of three helices and a three-stranded ß sheet.

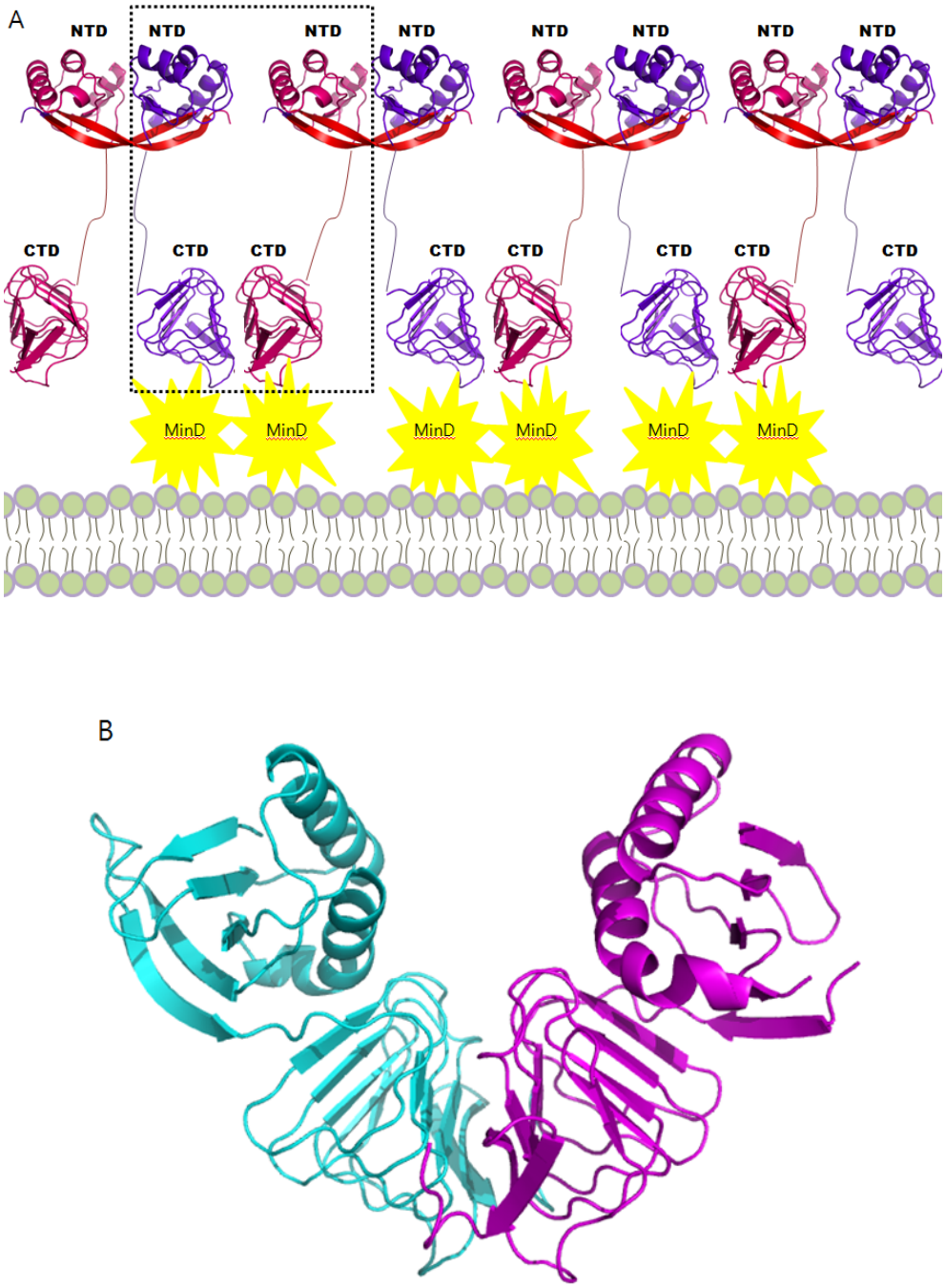

Fig. 3 (A) Putative polymer structure model of MinC from *E. coli*. black square area means dimer form of putative MinC structure. CTD region of MinC is modeled from *T. maritima* MinC. (B) Structure of MinC(PDB code 1hf2) from *T. maritima*